A First-Principles Study of Electromigration in the Metallic Liquid State of GeTe and Sb_2Te_3 Phase-Change Compounds

M. Cobelli,[†,‡] *M. Galante,*[‡] *S. Gabardi,*[†] *S. Sanvito,*[‡] *and M. Bernasconi*[*,†]

†*Dipartimento di Scienza dei Materiali, Università di Milano-Bicocca, Via R. Cozzi 55, I-20125 Milano, Italy*

‡*School of Physics and CRANN, Trinity College Dublin 2, Ireland*

E-mail: marco.bernasconi@unimib.it

Abstract

In the reset process of phase-change memories, the active material is brought rapidly above its melting temperature by Joule heating. Atomic migration in the liquid state due to the high electric field can lead to alloy demixing and eventually to device failure. The electromigration force F responsible for ionic migration is proportional to the electric field E, via the effective charge Z^* ($F = eZ^*E$, where e is electron charge). The determination of Z^* is thus of great relevance for the electrothermal modeling of devices. We show that a direct first principles calculation of the effective charges in metallic liquids is possible by computing the atomic forces in the presence of both an electric field and an electronic current within a non-equilibrium Green's function method based on density functional theory. We present results on the effective charges for GeTe and Sb_2Te_3 in their liquid state obtained with a calculation including wind forces.

Introduction

Phase-change compounds are exploited in rewritable optical disk and, more recently, in electronic non-volatile memories, named phase-change memories (PCMs).[1] PCMs are emerging as the most mature technology for the realization of the so-called storage class memories, namely memories suitable to combine non-volatility and high density with cyclability and endurance near to those of dynamic random access memories.[2] This is assessed by the 3D XPoint crossbar technology (Optane memory) recently commercialized by Intel and Micron.[3] A PCM is a resistor made of a thin film of a phase-change compound, typically $Ge_2Sb_2Te_5$ (GST)[1,4] or doped GeTe,[5,6] with a low-field resistance that changes by about three orders of magnitude across a fast and reversible transformation between the crystalline and amorphous phases. Joule heating induces amorphization via crystal melting (reset) or recrystallization of the amorphous phase (set). The amorphous-crystal transformation is very fast (2-100 ns, depending on the memory cell size) and highly reversible, providing cyclability in excess of 10^{12} in particular geometries.[7]

One of the critical issue for the scalability of PCM is the possibility of demixing or change in the composition of the ternary compound that occurs in the metallic liquid state under high electric fields during the reset operation. Direct evidence of alloy demixing under high electric fields in $Ge_2Sb_2Te_5$ has been provided by transmission electron microscopy (TEM).[8–11] These electromigration effects cause reliability problems and eventually device failure.[7,11,12] Some solutions have been proposed to mitigate these effects such as the application of occasional pulses with a reversed polarity.[13,14] More recently, it has been shown that the design of a more symmetrical cell ensures that a pore with a programmable composition can stay at the center of the cell after repeated cycling while the extremely segregated regions near the top and bottom electrodes simply act as extended electrodes.[7,15,16] The study of the microscopic mechanisms that control the electromigration process in the liquid metallic state of phase change materials is thus of great technological relevance.

During electromigration an atom feels an electromigration force F, which consists of

two terms: 1) a direct electrostatic term due to the electric field, and 2) a wind force term due to the scattering of the electrons in presence of the electrical current.[17] The total electromigration force is then proportional to the electric field E, and the relation $F = eZ^*E$ defines the effective charge Z^* (e is the electron charge).[17]

Effective charges in phase change materials have been recently estimated in an indirect way by modelling the concentration profile of the different species measured by TEM in highly cycled PCM cells.[12,18–20] In PCMs the concentration profile depends, in addition to electromigration forces, on terms due to the presence of thermal and stress gradients. When these contributions are taken into account the solution of the transport equation presented in Ref. [19] provides an estimate of the effective charges in molten GST, which reads Z^*_{Ge}= 0.55, Z^*_{Sb}= 0.65 and Z^*_{Te}= - 0.6. Similar values for the effective charges can be inferred from the measurements of Ref.[12] once the same diffusion coefficients of Ref. [19] are used. Unfortunately, these experimental estimates of Z^* rest on several, mostly unknown parameters that have been used in the phenomenological transport equations exploited to model the concentration profile as a function of the applied electric pulses. Moreover, in case of $Ge_2Sb_2Te_5$ incongruent melting during cycling could also lead to change in composition.[21] As such the experimental estimate of Z^* suffer from a significant uncertainty. Thus, a more direct estimation of Z^*, as that obtainable by first principles simulations, is much needed for the electrothermal modelling of the device in the reset operation.

In this work, we report on the calculation of the effective charges in the liquid state of GeTe and Sb_2Te_3 compounds which are the parent binary systems of the GST alloy used in PCMs. To this end, we have combined density functional theory (DFT) with the non-equilibrium Green's functions formalism (NEGF+DFT)[22–24] to compute the forces acting on the ions in the presence of a stationary electrical current in the ballistic regime.[25] It is then possible to obtain the effective charges by computing the forces on the ions for different values of the applied bias. This scheme has been applied previously to study the effective charges in crystalline materials,[26] but never in metallic liquids. Crystalline GeTe, Sb_2Te_3 and

GST are small gap semiconductors, while in their liquid phase they display a large density states associated to delocalized electrons at the Fermi level, E_F, as shown by DFT electronic structure calculations.[27–29] The density of delocalized states at E_F increases with temperature leading to a metallic-like conductivity. However, since the electrical conductivity increases with temperature these systems are still referred to as semiconductor liquids.

Computational Details

Our calculations proceed as follows. We have first generated models of liquid GeTe at 1020 K and liquid Sb_2Te_3 at 920 K by means of DFT molecular dynamics simulations in the Born-Oppenheimer approximation. These temperatures are close to the experimental melting temperature at normal conditions of GeTe (998 K)[30] and Sb_2Te_3 (890 K).[31] The quantum-espresso[32] suite was used together with norm-conserving pseudopotentials, a plane waves expansion of the Kohn-Sham orbitals up to a 20 Ry energy cutoff and the Perdew-Burke-Ernzerhof (PBE) exchange and correlation functional.[33] The liquid phase has been modeled in a supercell containing 64 atoms for GeTe and 65 atoms for Sb_2Te_3 in a prismatic geometry elongated along the z axis. The geometry is chosen in such a way that the liquid model could be inserted between two electrodes of crystalline aluminum by keeping periodic boundary conditions in the xy plane. The primitive vectors of the supercell are given in Tables I and II of the Supporting Information (SI). They correspond to the experimental density of the liquid at the melting point, namely 0.0335 atoms/Å^3 for GeTe[34] and 0.0281 atoms/Å^3 for Sb_2Te_3.[31] The Brillouin Zone (BZ) is sampled with a 2×2 uniform mesh in the xy plane. The total pair correlation function of our model of GeTe is compared in Fig. S1 of the SI with that of a larger 216-atom model taken from Ref.[35] The comparison demonstrates that the main structural features of liquid GeTe are already captured by our small simulation cell. A similar comparison for Sb_2Te_3 is shown in Fig. S2 in the SI.

The cell describing the liquid phase is then sandwiched between two metallic Al elec-

trodes in the two-terminal device setup used for the NEGF+DFT simulations. Here, we are interested in computing the forces acting on atoms at the center of the liquid model far from the electrodes. As such a full optimization of the interface between the crystalline electrodes and the liquid GeTe is not necessary, provided that an electrical coupling sufficient to drive the current is established between the electrodes and the liquid metal. The two Al electrodes are built with the [111] direction aligned with the z direction of the supercell (the direction of the current flow). By stacking the (111) planes of Al along z, a 3×3 hexagonal cell in the xy plane is built corresponding to a total of 54 atoms in each electrode. Thus, the Al/GeTe/Al and Al/Sb_2Te_3/Al models finally contain a total 172 and 173 atoms, respectively. A distance between the terminal planes of the electrodes of 33.216 Å is chosen in such a way to accommodate the GeTe atoms at the experimental liquid density of 0.0335 atoms/Å^3 and to include an Al interplanar distance along the [111] direction (2.343 Å). Analogously, a distance between the two electrode of 40.729 Å is chosen for the Al/Sb_2Te_3/Al model. The primitive lattice parameters in the xy plane are the same as those of the bulk liquid models (see Tables I and II in SI). A snapshot of the Al/GeTe/Al model is shown in Fig. 1, while that for Al/Sb_2Te_3/Al is shown in Fig. S3 of the SI.

The NEGF+DFT simulations have been then performed by using the Smeagol code,[23,24] which implements the NEGF formalism with the DFT framework of the Siesta code.[36] Norm conserving pseudopotentials and the PBE functional have been used, together a 5×5×1 uniform k-point mesh for BZ integration. A double-zeta-valence-plus-polarization (DZVP) basis set has been used. We remark that the forces computed with Siesta at zero bias are slightly different from the forces computed with Quantum-Espresso which is the code used to generate the liquid models. However, for the calculation of the effective charges we considered only differences in the forces with and without the electric field. This difference is computed on several configurations that are representative of the liquid phase irrespective of the code used to generate them.

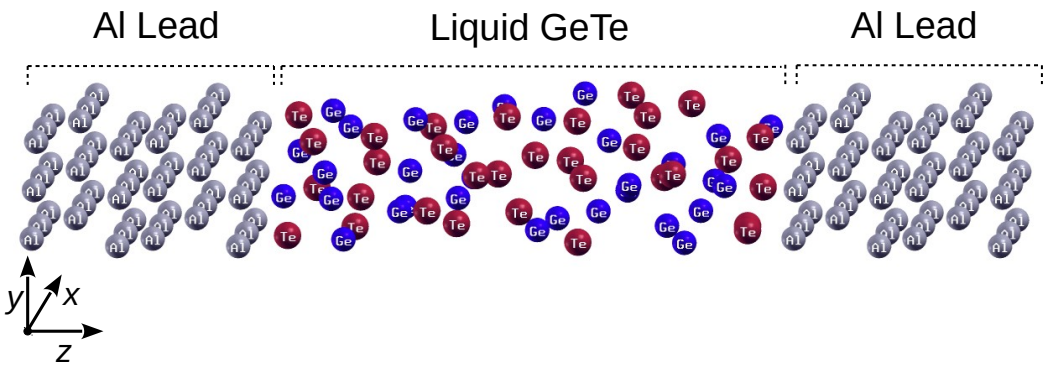

Figure 1: Atomic model of the Al/GeTe/Al junction used for the NEGF+DFT calculations. The model is made of 64 atoms of GeTe and 108 atoms of Al in the two leads.

Results and Discussion

By applying a finite bias between the electrodes, the NEGF formalism provides the self-consistent charge density in the presence of a steady-state electric current and the total forces acting on each ion as described in Ref. [25]. The electromigration forces, containing both direct and wind contributions, are then obtained as the difference between the forces at finite and at zero bias. In order to obtain a relation between the electromigration forces and the electric field, we have computed the self-consistent total electrostatic potential averaged over planes perpendicular to the z axis. An example is given in Fig. 2 for a single model of liquid GeTe and Sb_2Te_3. Similar plots for the same single models at different bias in the range 0.1-0.3 V are given in Fig. S4 of the SI.

The electric field averaged over planes perpendicular to the direction of the current can be reliably computed from the slope of the plane-averaged electrostatic potential (see Fig. 2). An estimate of Z^* is then obtained by taking the ratio between the electromigration forces F, and the electric field E, because a linear dependence between these two quantities was

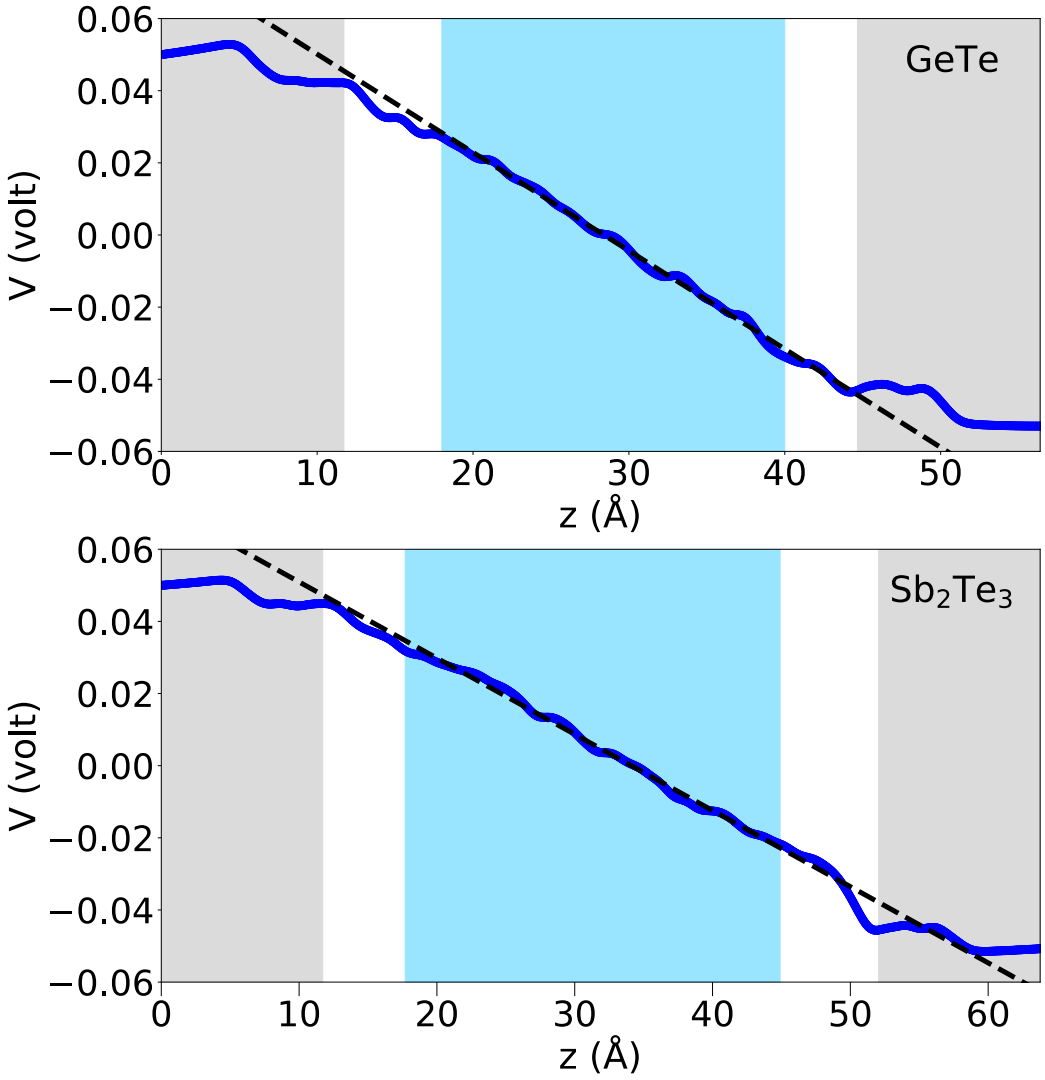

Figure 2: Profile of the planar average of the electrostatic potential as a function of the position along the z direction in a representative Al/GeTe/Al model (upper panel) and Al/Sb_2Te_3/Al model (lower panel). The shaded area at the edges correspond to the two Al electrodes, while that in the center corresponds to the region far from the electrodes, where a nearly constant planar averaged electric field is found. This region contains 51 atoms in the Al/GeTe/Al model and 52 atoms in the Al/Sb_2Te_3/Al one. The external bias between the two electrodes is 0.1 V for both the models.

actually found, as we will discuss below. In order to estimate the effective charges we have considered only atoms in the central region far from the electrodes, where a nearly uniform average electric field is present. This region is shown as a dashed light-blue area in Fig. 2 and contains 51 and 52 atoms, respectively for the Al/GeTe/Al and the Al/Sb_2Te_3/Al model.

In the central region the electronic structure at zero bias is only marginally affected by the presence of the electrode as shown in Fig. S5 of the SI, which reports the electronic density of states projected on the central region atoms for a single Al/GeTe/Al model compared to that of bulk GeTe (216-atom cubic cell). However, it is important to note that the atoms in the liquid are all in slightly different local configurations and they experience different local currents and a different response to the electric field. As an example of the variability of the electromigration force, a map of the forces acting on individual atoms projected on the xz plane is shown in Fig. 3. Similar maps for the Al/GeTe/Al model at different bias and for the Al/Sb_2Te_3 model are shown in Fig. S6-S7 of the SI.

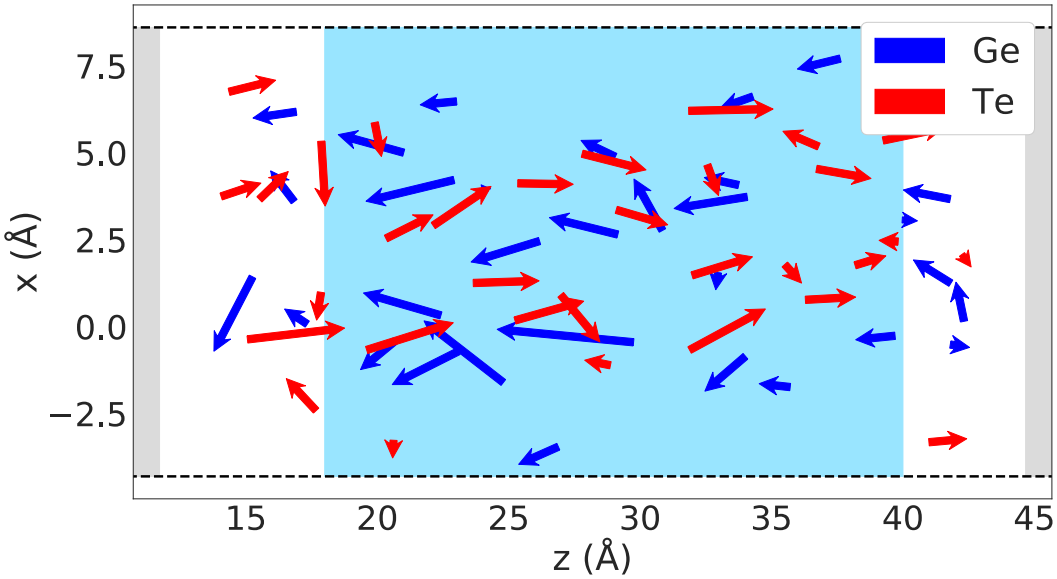

Figure 3: Map of the electromigration forces taken as the difference of the forces computed at zero and finite bias on individual atoms. The projection of the forces on the xz plane is shown for a representative Al/GeTe/Al model at 0.1 V (same as in Fig.2). Only atoms in the central region (shaded area), where the plane-averaged electric field is approximatively uniform, are considered in the calculation of Z^*.

A reliable estimate of the average effective charges was obtained by repeating the calculations for 13 inequivalent models presenting different atomic configurations extracted from the molecular dynamics trajectories for the bulk liquid. We then computed for each model the average electromigration forces over all atoms and the average electric field for different

bias as described above. The data are collected in Fig. 4 for three representative models and for the two different species in GeTe and Sb_2Te_3. Each point in Fig. 4 corresponds to the average force of a different model, while the error bar represents the spread in the values of the electromigration forces in each model for atoms belonging to the suitably chosen central region. The corresponding plots for the other ten GeTe and Sb_2Te_3 models are reported in Fig. S8 in the SI. The magnitude of the electric field is in the range 25-200 mV/nm, which is comparable to the values expected during the reset process of ultrascaled memories. The Z^* value is extracted for each model from the linear regression of the data in Fig. 4. The effective charges are then averaged over the 13 configurations yielding the values collected in Table 1 together with their mean square deviations.

The total charge per formula unit is obtained as $Z^*_{\rm fu}=Z^*_{\rm Ge}+ Z^*_{\rm Te}$ or $Z^*_{\rm fu}=2Z^*_{\rm Sb}+ 3Z^*_{\rm Te}$ and it is reported in Table 1. The total charge is very close to zero or even sightly positive, a fact suggesting that the wind force is very small in these systems. In general, the wind force is indeed expected to be much lower in liquid metals than in crystalline metals due to the lower electrical conductivity of the former.

Table 1: Effective charges for liquid GeTe at 1020 K and liquid Sb_2Te_3 at 920 K. The total charge per formula unit is given in the last column and it is obtained by summing the atomic charges.

	Z^*			
	Ge	Te	Sb	charge/f.u.
GeTe	3.65 ± 0.3	-3.69 ± 0.3	-	-0.05 ± 0.4
Sb_2Te_3	-	-2.39 ± 0.2	4.04 ± 0.2	0.89 ± 0.7

The resulting theoretical values of Z^* reported in Table 1 are about a factor six higher than those obtained for GST by modelling the experimental evolution of the concentration profile of the different species upon application of an electric current.[19] Since we do not expect the effective charges to change dramatically between the two binary compounds studied here and the ternary GST, our NEGF+DFT results suggest that electromigration, and thermal and stress gradients might have a different share in ionic migration than proposed in Ref.[19] . Another work aiming at disentangling the different contributions to compositional changes

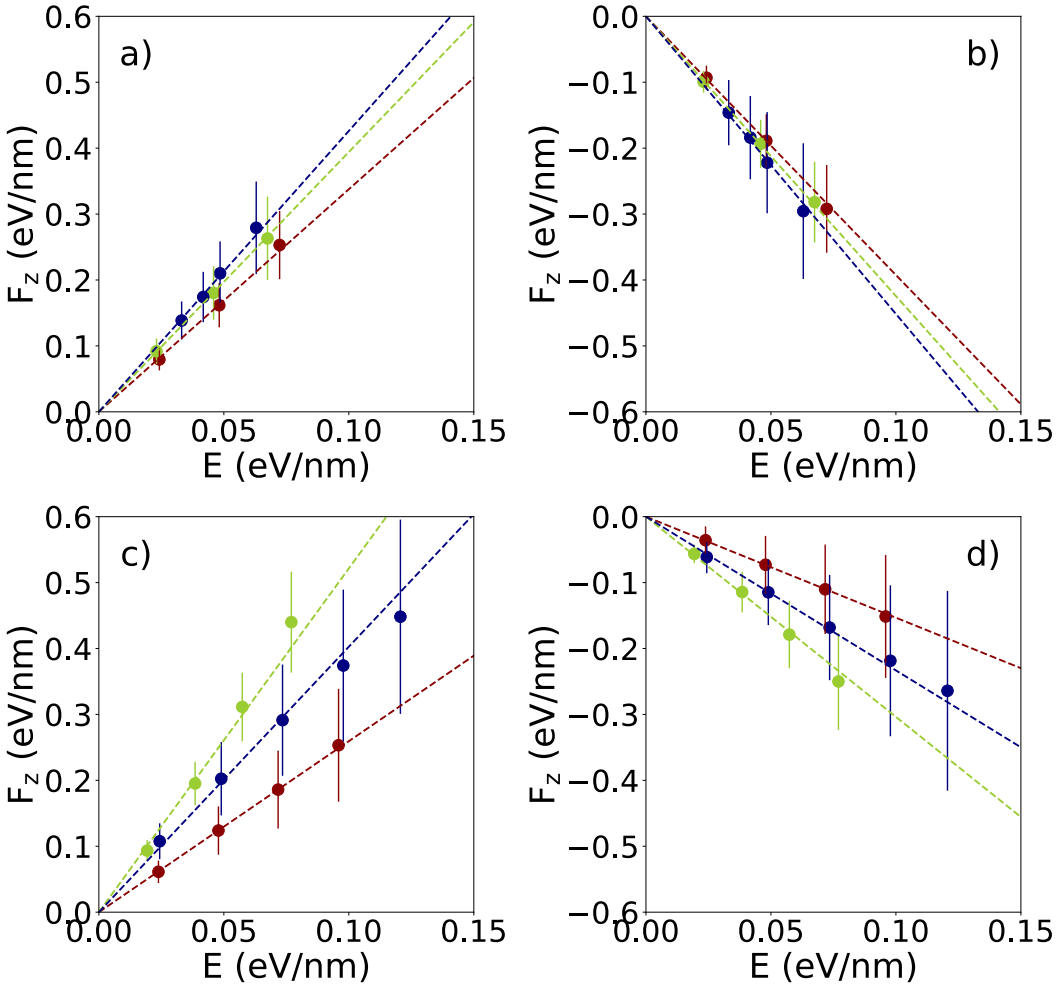

Figure 4: Electromigration forces as a function of electric field for a) Ge atoms in GeTe, b) Te atoms in GeTe, c) Sb atoms in Sb_2Te_3 and d) Te atoms in Sb_2Te_3 for three independent models. Each point is the result of the average over all atoms in the central region of a single model, i.e. for a single configuration of the liquid. The error bar represents the spread in the values of the electromigration forces for the different atoms in a single model. Different colors correspond to different models.

in cycled PCM came recently by Yeoh *et al* [37] who developed a methodology for isolating thermal-gradient effects without interference from electromigration due to the electric field. These measurements suggest that the Soret coefficients for thermodiffusion are similar in magnitude for Sb and Te atoms as opposed to a ratio of twenty resulting from the modeling of Ref.[19]

Conclusions

In conclusion, we have provided an *ab initio* evaluation of the effective charges in liquid GeTe and Sb_2Te_3, the two parental compounds of the pseuodbinary $Ge_2Sb_2Te_5$ alloy exploited in PCMs. By means of a NEGF-DFT method we have computed the forces acting on the various species and the average electric field, so that the effective charges have been estimated directly at the microscopic level. This allowed us to single out the electromigration contribution to the ionic motion that occurs during cell programming from those arising from temperature and stress gradients. As such our estimates provide a crucial starting point for the construction of electromigration models for real devices, a key tool for designing high-performance memories.

Acknowledgement

We thankfully acknowledge the computational resources provided by the ISCRA program at Cineca (Casalecchio di Reno, Italy). MG and SS thank Science Foundation Ireland (grant 14/IA/2624) and the Irish Research Council Advanced Laureate Award (IRCLA/2019/127) for financial support.

Supporting Information Available

We provide Supporting Information on the electronic and structural properties of the Al/GeTe/Al and Al/Sb_2Te_3/Al junctions.

References

(1) Wuttig, M.; Yamada, N. Phase-change materials for rewriteable data storage. *Nat. Mater.* **2007**, *6*, 824-832.

(2) Fong, S. W.; Neumann, C.M.; Wong, H.-S. P. Phase-change cemory - towards a storage-slass memory. *IEEE Trans. Electron. Dev.* **2017**, *64*, 4374-4385.

(3) Choe, J. Intel 3D XPoint memory die removed from Intel Optane PCM (Phase Change Memory). *TechInsights* **2017**, http://www.techinsights.com/about-techinsights/overview/blog/intel-3D-xpoint-memory-die-removed-from-intel-optane-pcm.

(4) Pirovano, A.; Lacaita, A. L.; Benvenuti, A.; Pellizzer, F.; Bez, R. Electronic switching in phase-change memories. *IEEE Trans. Electron. Dev.* **2004**, *51*, 452-459.

(5) Noé, P.; Vallée, C.; Hippert, F.; Fillot, F.; Raty, J.-Y. Phase-change materials for non-volatile memory devices: from technological challenges to materials science issues. *Semicond. Sci. Technol.* **2018**, *33*, 013002.

(6) Ghezzi, G. E. ; Raty, J.-Y.; Maitrejean, S.; Roule, A.; Elkaimand, E.; Hippert, F. Effect of carbon doping on the structure of amorphous GeTe phase change material. *Appl. Phys. Lett.* **2011**, *99*, 151906.

(7) Kim, W.; Burr, G.; Kim, W.; Nam, S.-W. Phase-change memory cycling endurance. *MRS Bull.* **2019**, *44*, 710-714.

(8) Kim, C.; Kang, D.; Lee, T.-Y.; Kim, K. H. P.; Kang, Y.-S.; Lee, J.; Nam, S.-W.; Kim, K.-B.; Khang, Y. Direct evidence of phase separation in $Ge_2Sb_2Te_5$ in phase change memory devices. *Appl. Phys. Lett.* **2009**, *94*, 193504.

(9) Kang, D.; Lee, D.; Kim, H.-M.; Nam, S.-W.; Kwon, M.-H.; Kim, K.-B. Analysis of the electric field induced elemental separation of $Ge_2Sb_2Te_5$ by transmission electron microscopy. *Appl. Phys. Lett.* **2009**, *95*, 011904.

(10) Padilla, A.; Burr, G. W. ; Rettner, C. T.; Topuria, T.; Rice, P. M. ; Jackson, B.; Virwani, K.; Kellock, A. J.; Dupouy, D.; Debunne, A.; *et al.* Voltage polarity effects in $Ge_2Sb_2Te_5$-based phase change memory devices. *J. Appl. Phys.* **2011**, *110*, 054501.

(11) Huang, Y.-H.; Hang, C.-H.; Huang, Y.-J.; Hsieh, T.-E. Electromigration behaviors of $Ge_2Sb_2Te_5$ chalcogenide thin films under DC bias. *J. Alloys Compd.* **2013**, *580*, 449-456.

(12) Yang, T.-Y.; Park, I.-M.; Kim, B.-J.; Joo, Y.-C. Atomic migration in molten and crystalline $Ge_2Sb_2Te_5$ under high electric field. *Appl. Phys. Lett.* **2009**, *95*, 032104.

(13) Lee, S.; Jeong, J.-H.; Lee, T. S.; Kim, W. M.; Cheong, B.-K. A novel programming method to refresh a long-cycled phase change memory cell. *Joint Non-Volatile Semiconductor Memory Workshop and International Conference on Memory Technology and Design (IEEE), Opio, France* **2008**, 4648.

(14) Goux, L.; Tio Castro, D.; Hurkx, G. A. M.; Lisoni, J. G.; Delhougne, R.; Gravesteijn, D. J.; Attenborough, K.; Wouters, D.J. Degradation of the reset switching during endurance testing of a phase-change line cell. *IEEE Trans. Electron Devices* **2009**, *56*, 354-358.

(15) Kim, W.; BrightSky, M.; Masuda, T.; Sosa, N.; Kim, S.; Bruce, R.; Carta, F.; Fraczak, G.; Cheng, H.-Y.; Ray, A.; *et al.* ALD-based confined PCM with a metallic liner toward unlimited endurance. *IEEE International Electron Devices Meeting (IEDM), San Francisco, CA* **2016**, 4.2.1-4.2.4.

(16) Kim, W.; Kim, S.; Bruce, R.; Carta, F.; Fraczak, G.; Ray, A.; Lam, C.; BrightSky, M.; Zhu, Y.; Masuda, T.; *et al.* Reliability benefits of a metallic liner in confined PCM *IEEE International Reliability Physics Symposium (IRPS), IEEE, Burlingame, CA* **2018**, 6D.5-16D.5-5.

(17) Kandel, D.; Kaxiras, E. Microscopic theory of electromigration on semiconductor surfaces. *Phys. Rev. Lett.* **1996**, *76*, 1114-1117.

(18) Yang, T.-Y.; Cho, J.-Y.; Park, Y.-J.; Joo, Y.-C. Driving forces for elemental demixing of GeSbTe in phase-change memory: computational study to design a durable device *Current Applied Physics* **2013**, *13*, 1426-1432.

(19) Crespi, L.; Lacaita, A. L.; Boniardi, M.; Varesi, E.; Ghetti, A.; D'Arrigo, A. G. Modeling of atomic migration phenomena in phase change memory devices. *IEEE 7th International Memory Workshop (IMW), Monterey, CA* **2015**, 22-25.

(20) Novielli, G.; Ghetti, A.; Varesi, E.; Mauri, A.; Sacco, R.; Atomic migration in phase change materials. *IEEE International Electron Devices Meeting (IEDM), Washington, DC* **2013**, 22.3.1-22.3.4.

(21) Nam, S.-W.; Kim, C.; Kwon, M.-H.; Lee, H.-S.; Wi, J.-S.; Lee, D.; Lee, T.Y.; Khang, Y.; Kim, K.-B. Phase separation behavior of $Ge_2Sb_2Te_5$ line structure during electrical stress biasing. *App. Phys. Lett.* **2008**, *92*, 111913.

(22) Sanvito, S.; Lambert, C. J.; Jefferson, J. H.; Bratkovsky, A. M. General Green's-function formalism for transport calculations with spd Hamiltonians and giant magnetoresistance in Co- and Ni-based magnetic multilayers. *Phys. Rev. B* **1999**, *59*, 11936.

(23) Rocha, A. R.; Garcia Suarez, V. M.; Bailey, S. W.; Lambert, C.J.; Ferrer J.; Sanvito, S. Spin and molecular electronics in atomically generated orbital landscapes. *Phys. Rev. B* **2006**, *73*, 085414.

(24) Rungger, I.; Sanvito, S. Algorithm for the construction of self-energies for electronic transport calculations based on singularity elimination and singular value decomposition. *Phys. Rev. B* **2008**, *78*, 035407.

(25) Zhang, R.; Rungger, I.; Sanvito, S.; Hou, S. Current-induced energy barrier suppression for electromigration from first principles. *Phys. Rev. B* **2011**, *84*, 085445.

(26) Bevan, K. H.; Guo, H.; Williams, E. D. ; Zhang, Z. First-principles quantum transport theory of the enhanced wind force driving electromigration on Ag(111). *Phys. Rev. B* **2010**, *81*, 235416.

(27) Raty, J. Y.; Godlevsky, V. V.; Gaspard, J. P.; Bichara, C.; Bionducci, M.; Bellissent, R.; Céolin, R.; Chelikowsky, J. R. Local structure of liquid GeTe via neutron scattering and ab initio simulations. *Phys. Rev. B* **2002**, *65*, 115205.

(28) Weber, H.; Schumacher, M.; Jóvári, P.; Tsuchiya, Y.; Skrotzki, W.; Mazzarello, R.; Kaban, I. Experimental and ab initio molecular dynamics study of the structure and physical properties of liquid GeTe. *Phys. Rev. B* **2017**, **96**, 054204.

(29) Caravati, S.; Bernasconi, M.; Parrinello, M. First-principles study of liquid and amorphous Sb_2Te_3. *Phys. Rev. B*, **2010**, *81*, 014201.

(30) Klemm, W.; Frischmuth, G. Das system germanium-tellur. *Z. Anorg. Chem.* **1934**, *218*, 249-251.

(31) Singh, K. J.; Satoh, R.; Tsuchiya, Y. Structural changes and compound forming effects in the molten SbTe system investigated by molar volume and sound velocity measurements. *J. Phys. Soc. Jpn.* **2003**, *72*, 2546-2550.

(32) Giannozzi, P.; Baroni, S.; Bonini, N.; Calandra, M.; Car, R.; Cavazzoni, C.; Ceresoli, D.; Chiarotti, G. L.; Cococcioni, M.; Dabo, I.; *et al.* QUANTUM ESPRESSO: a mod-

ular and open-source software project for quantum simulations of materials. *J. Phys.: Condens. Matter* **2009**, *21*, 395502; www.quantum-espresso.org.

(33) Perdew, J.P.; Burke, K.; Ernzerhof, M. Generalized gradient approximation made simple. *Phys. Rev. Lett.* **1996**, *77*, 3865-3868.

(34) Glazov, V. M.; Shelichov, O. D. Thermal-espansion and characteristics of the atomic vibrations in melts of IV-VI compounds. *Sov. Phys. Semicond.* **1984**, *18*, 411-413.

(35) Sosso, G. C.; Miceli, G.; Caravati, S.; Behler, J.; Bernasconi, M. Neural network interatomic potential for the phase change material GeTe. *Phys. Rev. B* **2012**, *85*, 174103.

(36) Soler, J. M.; Artacho, E.; Gale, J. D.; Garca, A.; Junquera, J.; Ordejon, P.; Daniel Sanchez-Portal, D. The SIESTA method for ab initio order-N materials simulation. *J. Phys. Condens. Matter* **2002**, *14*, 2745.

(37) Yeoh, P.; Cullen, D. A.; Bain, J. A.; Skowronski, M. Thermal-gradient-driven elemental segregation in $Ge_2Sb_2Te_5$ phase change memory cells. *Appl. Phys. Lett.* **2019**, *114*, 163507.

TOC graphic